Femtosecond Light Source for Phase-Controlled Multiphoton Ionization

A. V. Sokolov, D. R. Walker, D. D. Yavuz, G. Y. Yin, and S. E. Harris

Edward L. Ginzton Laboratory, Stanford University, Stanford, California 94305

We describe a femtosecond Raman light source with more than an octave of optical bandwidth. We use this source to demonstrate phase control of multiphoton ionization under conditions where ionization requires eleven photons of the lowest frequency of the spectrum or five photons of the highest frequency. The nonlinearity of the photoionization process allows us to characterize the light source. Experiment-to-theory comparison implies generation of a near single-cycle waveform.

PACS numbers: 42.50.Gy, 32.80.Qk, 42.60.Fc, 42.65.Dr

Over the past decade, advances in femtosecond mode-locked laser technology [1,2] have fueled a broad field of ultrafast physics and chemistry [3], and allowed coherent control of molecular dynamics [4]. Generation of subfemtosecond and single-cycle pulses would extend the horizon of ultrafast measurements to the time scale of electronic motion. In this Letter, we report a first step toward this goal: We describe a new source of ultrabroadband radiation [5,6], and use it to demonstrate phase control of multiphoton ionization on a few-femtosecond time scale.

Before proceeding, we note that other authors have proposed several methods for subfemtosecond pulse generation. These methods rely on phase locking a wide spectrum of equidistant frequency components, obtained from frequency mixing of separate phase-locked laser oscillators [7], high-order harmonic generation [8], or Raman scattering [9,10].

Our source is based on collinear generation of a wide spectrum of equidistant, mutually coherent Raman sidebands. The essence of this technique is the adiabatic (off-resonant) preparation of a macroscopic molecular ensemble in a single vibrational superposition state. When this is the case, highly coherent molecular motion modulates laser light and produces a wide FM-like spectrum, with a possibility of subfemtosecond pulse compression within the molecular medium itself [5]. In our experiment, the spectrum consists of seventeen sidebands and extends over many octaves of optical bandwidth, with energies above 1 mJ per 10 ns pulse for each of the nine central sidebands [6]. In the present work, we select a subset of five spectral sidebands with wavelengths ranging from 1.06 μm to 468 nm, and measure the ionization rate of xenon (Xe) as a function of the sideband phases.

Figure 1 shows our experimental setup. The experimental apparatus for collinear Raman generation is described in detail in Refs. [6,11]. We use two synchronized transform-limited laser pulses (typically 80 mJ/15 ns at a 10 Hz repetition rate) at wavelengths of 1.06 μm (fixed) and 807 nm (tunable). The laser frequency difference is tuned 0.6 GHz below the fundamental vibrational frequency in D_2 (2994 cm^{-1}). The laser beams are combined on a dichroic beam splitter and loosely focused into a D_2 cell (with a D_2 pressure of 38 torr). We disperse the cell out-

put spectrum with a prism and select five sidebands ranging from 1.06 μm in the infrared to 468 nm in the blue. Each sideband is retroreflected through the prism, such that the spectrum is recombined in a slightly offset beam, which is picked off by a small mirror [12]. Sideband energies in the combined beam are 33 mJ (at 1.06 μm), 28 mJ (at 807 nm), 4.2 mJ (at 650 nm), 0.9 mJ (at 544 nm), and 0.2 mJ (at 468 nm). We adjust sideband phases by tilted glass plates, and focus the recombined beam into low-pressure (3 × 10^{-5} torr) Xe gas.

The number of ions is measured with a Channeltron detector. Different chemical species are selected according to their masses, by measuring their time of flight from the laser focal point to the detector. Figure 2 shows the mass spectrum of ions produced by the multicolor beam. In addition to a distinct Xe peak, we observe several impurity peaks, with the largest of them attributed to carbon (C).
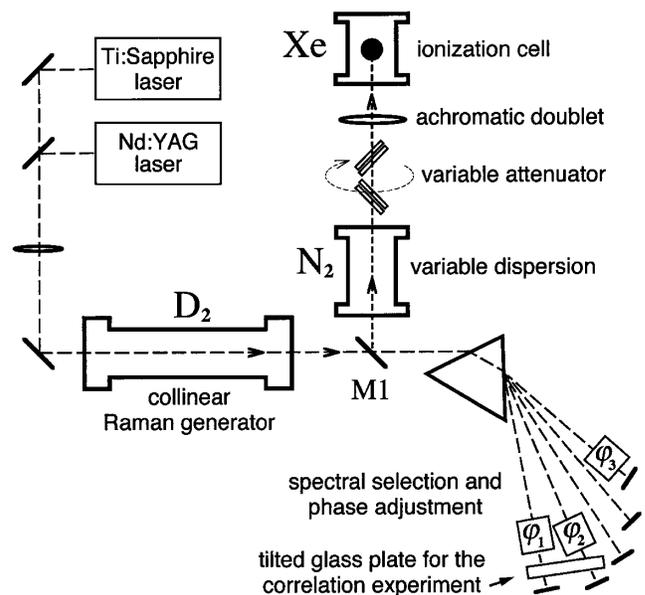

FIG. 1. Experimental setup for multiphoton ionization of Xe with five Raman sidebands (at 1.06 μm, 807 nm, 650 nm, 544 nm, and 468 nm). The mirror M1, which is displayed in the vertical plane, picks off the slightly offset retroreflected beam. We vary sideband phases independently with tilted glass plates, or by varying dispersion in the N_2 pressure cell.
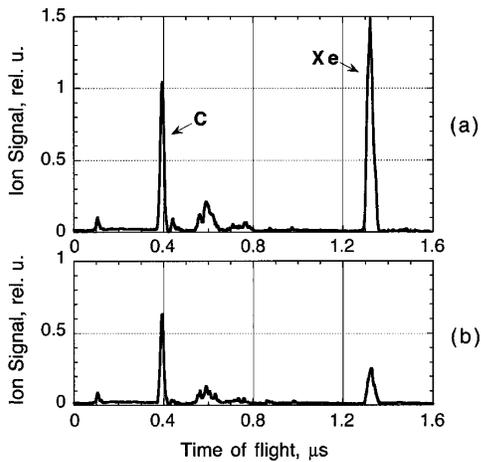
FIG. 2. Time-of-flight mass spectroscopy of the photoionized species, detected in the Xe cell in the setup of Fig. 1. In addition to a distinct Xe peak, we observe peaks that correspond to lighter species. Spectra (a) and (b) are recorded with sideband phases adjusted to maximize (a) or minimize (b) Xe ionization.
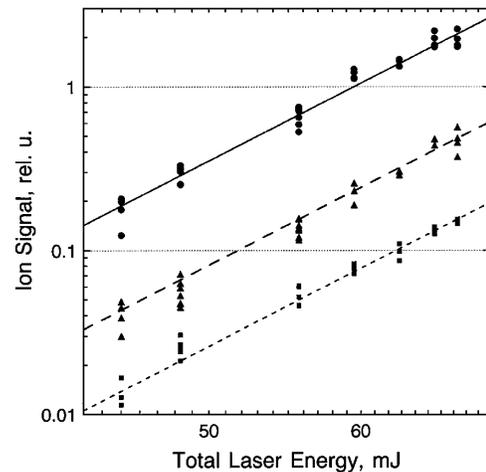

FIG. 3. Multiphoton ionization of Xe with spectral bandwidth such that the ionization requires eleven photons of the lowest frequency or five photons of the highest frequency. The ion yield is shown as a function of total energy in laser pulses. Three sets of data, which corresponds to different temporal pulse shapes, are all fitted by a sixth-order power law.

As we vary the relative phases of the five spectral components, the ratio of carbon to xenon changes by as much as a factor of 5. An example is shown in Fig. 2. Since the number of C ions is nearly unchanged as the number of Xe ions varies, we believe that the change in the Xe:C ratio is a result of the stronger dependence of Xe ionization rate on the peak electric field amplitude of the temporal waveform.

Next, in order to measure the ion yield as a function of the total applied laser energy (with relative spectral energies fixed as noted above), we use a wavelength-independent variable attenuator. The attenuator is composed of four fused-silica plain-parallel plates, inserted into the combined multicolor beam (Fig. 1) and tilted by approximately 45 degrees with respect to the beam. The plates are rotated around the axes of the beam to provide variable transmission for linearly polarized sidebands. For these conditions, the attenuation of different spectral components is approximately equal.

Figure 3 shows the dependence of the Xe ion signal on total pulse energy (summed over five sidebands). Three sets of data in the figure correspond to different relative phases among the sidebands, or equivalently, to different temporal shapes of the waveform. For Set 1 (circles), we adjust sideband phases to maximize the Xe signal (phase-locked spectrum). For Set 2 (squares), we change the phase of the 1.06 μm beam by π. For Set 3 (triangles), we return the phase of the 1.06 μm beam to its original value and change the phase of the 468 nm beam by π. For all three cases, the data fits well to a sixth-order power law [solid (Set 1), dashed (Set 2), and dotted (Set 3) lines in Fig. 3]. We estimate our experimental uncertainty for the order of the power law to be plus/minus one. We conclude that, at our experimental conditions, the sixth-order channel dominates in the photoionization process, with pos-

sible contributions from fifth- and seventh-order channels. The important observation is that, to the precision of our measurement, the order of the ionization process does not depend on the laser pulse shape. The ion yield, at a fixed laser energy, changes as a function of the temporal shape. But at a fixed pulse shape the slope of the ion signal versus laser energy (on a log-log scale) does not depend on the temporal structure.

We can now use the pulse-shape sensitivity of the photoionization to characterize our light source. We perform cross-correlation measurements, in a collinear configuration. We vary the delay of the 544 and 468 nm beams with respect to the 650 nm, 807 nm, and 1.06 μm beams. We do this by tilting a glass plate, which overlaps the 544 and 468 nm beams (Fig. 1). The result of this measurement is shown in Fig. 4 (solid line).

We compare this result with a simple calculation (dashed line). In this calculation, we assume that the applied electric field is a sum of five perfectly coherent monochromatic waves (with an arbitrary time origin): $E(t, \tau_5) = \sum_{m=1}^{5} \frac{1}{5} \cos[\omega_m(t + \tau_m)]$, where $\tau_1 = \tau_2 = \tau_3 = 0$, $\tau_4 = 0.93\tau_5$, and τ_5 is the variable time delay, which is calculated from the tilt angle of the glass plate. (When we tilt the plate, the time delay for the two beams is not the same, because of dispersion in glass, and also because of the fact that the two beams cross the plate at slightly different angles; the factor 0.93 accounts for this difference.) In our experiments, we have adjusted the intensities such that each frequency component contributes to the ion production approximately equally. Therefore it is reasonable to take the amplitudes of the five terms in the sum as equal. Furthermore, we assume an ideal sixth-order response of the atomic system and calculate the expected ion signal as $\int [E(t, \tau_5)]^{12} dt$. We observe a
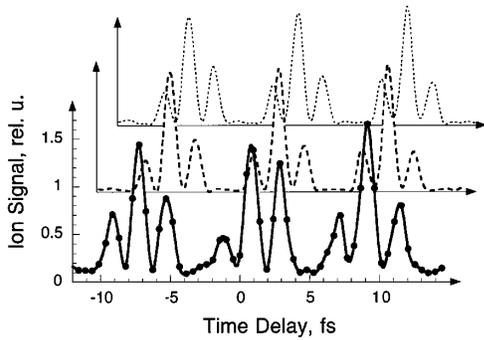
FIG. 4. Correlation of waveforms, synthesized by subsets of Raman sidebands: experiment (solid line), time domain calculation: $\int \{\sum \cos[\omega_m(t + \tau_m)]\}^{12}\, dt$ (dashed line), and perturbative frequency domain calculation (dotted line).
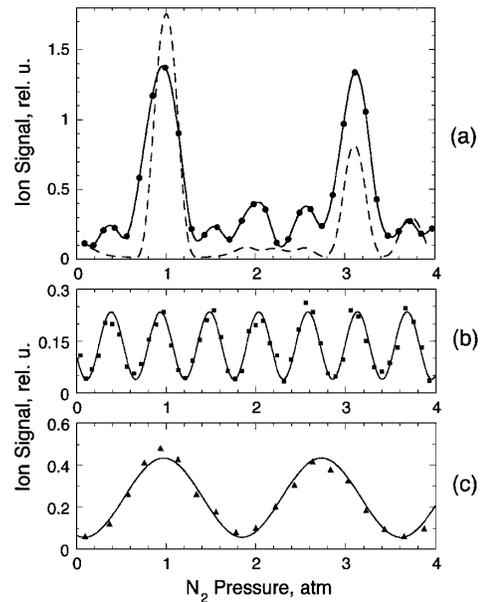

FIG. 5. Number of Xe ions produced in the setup in Fig. 1, versus pressure in the N_2 cell. For part (a) all five sidebands are present. For parts (b) and (c) we leave only three equidistant sidebands [1.06 μm, 650 nm, and 468 nm for part (b), and 650, 544, and 468 nm for part (c)]. The solid line is a cubic spline interpolation of the data in part (a) and a sinusoidal fit to the data in parts (b) and (c). The dashed line shows $\int [\sum \cos(\omega_m t + \varphi_m)]^{12}\, dt$, where φ_m are determined by N_2 dispersion. For the data in part (a), we observe significant saturation for ion signal above 1 relative unit (see text for details).

good qualitative agreement of our experimental data with this calculation.

We also perform a more rigorous frequency-domain calculation (dotted line in Fig. 4). In this calculation, we take experimental values for the sideband energies, and assume diffraction-limited focusing for each sideband. We perform a perturbative calculation of ionization probability and include all known Xe energy levels [13] and all possible ionization paths. Since the dipole matrix elements between Xe energy levels are not known, we assume that their relative values are equal. We normalize these matrix elements so that the total oscillator strength from each level to all other levels is approximately equal to unity. We observe good agreement between our two calculations (dashed and dotted lines in Fig. 4), and between the theory and the experiment. In the frequency-domain calculation, we also find, in rough agreement with our experimental data (Fig. 3), that the seventh-order process dominates, while sixth- and eighth-order processes have smaller but comparable contributions to the ionization of Xe.

To investigate the broadband nature of our waveform, and to further test the mutual coherence among the sidebands, we use variable dispersion. We put a gas cell (34 cm long) into the combined beam (just before the Xe cell, Fig. 1) and fill it with nitrogen gas (N_2). We adjust sideband phases such that the ion signal maximizes for 1 atm pressure, and count the number of Xe ions per laser shot as a function of N_2 pressure [Fig. 5(a)]. We observe a sharp decrease in the ion signal as the N_2 pressure changes. This is caused by dispersion in N_2. As the N_2 pressure changes by 2.2 atm, the dispersion is such that the sidebands rephase and the ion signal increases. We repeat this experiment for subsets of three equally spaced sidebands. We observe a nearly sinusoidal dependence of the ion signal on N_2 pressure [Figs. 5(b) and 5(c)] [14]. Note that the higher the frequency separation among the sidebands, the smaller the change in N_2 pressure is required to produce a π phase shift among them. The dashed line in Fig. 5(a) shows a result of the simple calculation:

$\int [\sum \cos(\omega_m t + \varphi_m)]^{12}\, dt$, where the phases φ_m are determined by N_2 pressure (frequency-dependent refractive index of N_2 is obtained from Ref. [15]).

The ion signal in Figs. 2 through 5 is given in relative units. One relative unit corresponds to (roughly) 42 ions per laser shot, produced at 3×10^{-5} torr Xe pressure. Each data point is averaged over 80 laser shots for Figs. 2, 4, 5(a), and 5(b), and over 160 shots for Figs. 3 and 5(c). For the conditions of our photoionization experiment, we estimate the focal volume to be roughly 10^{-4} mm^3, such that at 3×10^{-5} torr pressure the number of Xe atoms in the focal region is $\approx 10^5$. In order to increase the dynamic range of ion detection, we vary Xe pressure and normalize the signal to Xe concentration. According to our calculations, the ionization rate, which corresponds to one relative unit in our plots, is on the order of $3 \times 10^{-4}/(10\ \text{ns})$.

It is known that a phase-locked spectrum with a bandwidth equal to one octave, corresponds to single-cycle pulses. In the past, single-cycle (and subcycle) pulses were available only in the THz spectral region, with a duration of about 0.5 ps [16]. The experimental results, presented in this Letter (in particular, high contrast of the ion signal in Figs. 2 through 5, and the theory/experiment agreement), establish evidence for a good mutual coherence among frequency components, which extend over an octave of optical bandwidth, and prove our ability to phase lock these

components. Thus, we infer that in this experiment we are able to synthesize trains of single-cycle pulses (with a repetition period of 11 fs and a pulse duration of 2 fs).

Trains of single-cycle pulses can be used to study the dependence of photoionization on the optical phase of the pulse under the envelope. In such an experiment, the signal from all pulses in the train will add coherently. To produce trains of identical pulses, it will be necessary to use driving lasers at frequencies equal to a multiple of their frequency difference [17].

In summary, this Letter shows that the new type of a Raman source can be used to study multiphoton ionization in a regime not accessible by other light sources. Our experiment explicitly demonstrates the following: (1) good mutual coherence among the multiple sidebands as they are generated; (2) the ability to adjust individual phases, with small phase drifts; and (3) the ability to focus the multicolor beam tightly to achieve required intensities, with good beam pointing stability. Furthermore, we demonstrate that phase-controlled multiphoton ionization provides a tool for measuring ultrashort pulses. From indirect measurements, we infer generation of a near single-cycle waveform. In future experiments, we plan to use photoionization to further characterize the generated pulse shape by measuring its temporal autocorrelation function, and to extend our photoionization experiments to the subfemtosecond domain.

[1] Modern self-mode-locked Ti:sapphire lasers produce 10 fs pulses at 100 MHz repetition rates: J. Zhou, G. Taft, C.-P. Huang, M. M. Murnane, H. C. Kapteyn, and I. P. Christov, Opt. Lett. **19**, 1149 (1994); A. Stingl, M. Lenzner, Ch. Spielmann, F. Krausz, and R. Szipocz, Opt. Lett. **20**, 602 (1995); A. Kasper and K. J. Witte, Opt. Lett. **21**, 360 (1996).

[2] The shortest optical pulses generated to date (4.5 fs) are obtained by expanding the spectrum of a mode-locked laser by self-phase modulation in an optical waveguide, and then compensating for group velocity dispersion by diffraction grating and prism pairs: R. L. Fork, C. H. Brito-Cruz, P. C. Becker, and C. V. Shank, Opt. Lett. **12**, 483 (1987); A. Baltuska, Z. Wei, M. S. Pshenichnikov, and D. A. Wiersman, Opt. Lett. **22**, 102 (1997); M. Nisoli, S. DeSilvestri, O. Svelto, R. Szipocs, K. Ferencz, Ch. Spielmann, S. Sartania, and F. Krausz, Opt. Lett. **22**, 522 (1997).

[3] P. Corkum, Opt. Photonics News **6**, 18 (1995); F. Krausz, T. Brabec, M. Schnurer, and C. Spielmann, Opt. Photonics News **9**, 46 (1998).

[4] S. A. Rice and M. Zhao, *Optical Control of Molecular Dynamics* (Wiley, New York, 2000); M. Shapiro and P. Brumer, Adv. At. Mol. Opt. Phys. **42**, 287 (2000).

[5] S. E. Harris and A. V. Sokolov, Phys. Rev. Lett. **81**, 2894 (1998); A. V. Sokolov, D. D. Yavuz, and S. E. Harris, Opt. Lett. **24**, 557 (1999); A. V. Sokolov, Opt. Lett. **24**, 1248 (1999).

[6] A. V. Sokolov, D. R. Walker, D. D. Yavuz, G. Y. Yin, and S. E. Harris, Phys. Rev. Lett. **85**, 562 (2000).

[7] T. W. Hansch, Opt. Commun. **80**, 71 (1990).

[8] Gy. Farcas and Cs. Toth, Phys. Lett. A **168**, 447 (1992); S. E. Harris, J. J. Macklin, and T. W. Hansch, Opt. Commun. **100**, 487 (1993); P. Antoine, A. L.'Huiller, and M. Lewenstein, Phys. Rev. Lett. **77**, 1234 (1996); K. J. Schafer and K. C. Kulander, Phys. Rev. Lett. **78**, 638 (1997); I. P. Christov, M. M. Murnane, and H. C. Kapteyn, Phys. Rev. Lett. **78**, 1251 (1997); P. B. Corkum, N. H. Burnett, and M. Y. Ivanov, Opt. Lett. **19**, 1870 (1994).

[9] S. Yoshikawa and T. Imasaka, Opt. Commun. **96**, 94 (1993); H. Kawano, Y. Hirakawa, and T. Imasaka, IEEE J. Quantum Electron. **34**, 260 (1998); A. E. Kaplan, Phys. Rev. Lett. **73**, 1243 (1994); A. E. Kaplan and P. L. Shkolnikov, J. Opt. Soc. Am. B **13**, 347 (1996); M. Wittmann, A. Nazarkin, and G. Korn, Phys. Rev. Lett. **84**, 5508 (2000).

[10] There has been related work on dynamics of a single intense laser pulse in a Raman-active medium: E. M. Belenov, A. V. Nazarkin, and I. P. Prokopovich, Pis'ma Zh. Eksp. Teor. Fiz. **55**, 223 (1992) [JETP Lett. **55**, 218 (1992)]; E. M. Belenov, P. G. Kryukov, A. V. Nazarkin, and I. P. Prokopovich, Zh. Eksp. Teor. Fiz. **105**, 28 (1994) [Sov. Phys. JETP **78**, 15 (1994)].

[11] A. V. Sokolov, D. D. Yavuz, D. R. Walker, G. Y. Yin, and S. E. Harris, Phys. Rev. A **63**, 051801 (2001).

[12] In essence, we utilize the simplest version of the spectral modification technique: C. W. Hillegas, J. X. Tull, D. Goswami, D. Strickland, and W. S. Warren, Opt. Lett. **19**, 737 (1994); A. M. Weiner, Prog. Quantum Electron. **19**, 161 (1995); T. Baumert, T. Brixner, V. Seyfried, M. Strehle, and G. Gerber, Appl. Phys. B **65**, 779 (1997).

[13] Atomic Energy Levels, NSRDS-NBS 35 Volume III (1971).

[14] This result is related to the work on phase control of multiphoton excitations using a second or a third harmonic together with the fundamental laser frequency [for references, see R. A. Blank and M. Shapiro, Phys. Rev. A **52**, 4278 (1995); M. Protopapas, C. H. Keitel, and P. L. Knight, Rep. Prog. Phys. **60**, 454 (1997)]. In our experiment, where the frequencies are equally spaced but not commensurate, a minimum of three sidebands is required to achieve phase control.

[15] E. C. Craven, Proc. Phys. Soc. London **57**, 97 (1945).

[16] R. R. Jones, D. You, and P. H. Bucksbaum, Phys. Rev. Lett. **70**, 1236 (1993).

[17] The ability to control the phase of the optical oscillation under the envelope of few-cycle pulses was recently demonstrated in an experiment with a mode-locked laser: A. Apolonski, A. Poppe, G. Tempea, Ch. Spielmann, Th. Udem, R. Holzwarth, T. W. Hansch, and F. Krausz, Phys. Rev. Lett. **85**, 740 (2000).